

Bound states and superconductivity in dense Fermi systems

D. Blaschke^{1,2} and D. Zablocki^{1,3}

¹ *Instytut Fizyki Teoretycznej, Uniwersytet Wrocławski, 50-204 Wrocław, Poland*

² *Bogoliubov Laboratory for Theoretical Physics, JINR, 141980 Dubna, Russia*

³ *Institut für Physik der Universität, D-18051 Rostock, Germany*

Abstract

A quantum field theoretical approach to the thermodynamics of dense Fermi systems is developed for the description of the formation and dissolution of quantum condensates and bound states in dependence of temperature and density. As a model system we study the chiral and superconducting phase transitions in two-flavor quark matter within the NJL model and their interrelation with the formation of quark-antiquark and diquark bound states. The phase diagram of quark matter is evaluated as a function of the diquark coupling strength and a coexistence region of chiral symmetry breaking and color superconductivity is obtained at very strong coupling. The crossover between Bose-Einstein condensation (BEC) of diquark bound states and condensation of diquark resonances (Cooper pairs) in the continuum (BCS) is discussed as a Mott effect. This effect consists in the transition of bound states into the continuum of scattering states under the influence of compression and heating. We explain the physics of the Mott transition with special emphasis on role of the Pauli principle for the case of the pion in quark matter.

PACS: 11.10.St, 12.38.Lg, 21.65.Qr

1 Introduction

Key issues of modern physics of dense matter are concepts explaining the phenomena related to the appearance of quantum condensates in dense Fermi systems. Two regimes are well-known: the Bose-Einstein condensation (BEC) of bound states with an even number of Fermions and the condensation of bosonic correlations (e.g., Cooper pairs) in the continuum of unbound states according to the Bardeen-Cooper-Schrieffer (BCS) theory. While the former mechanism concerns states which are well-localized in coordinate space as they occur for strong enough attractive coupling, the latter mechanism applies to states which are correlated within a shell of the order of the energy gap Δ around the Fermi sphere in momentum space but delocalized in coordinate space. The transition between both regimes is called BEC-BCS crossover. Recently, this transition regime became accessible to laboratory experiments with ultracold gases of fermionic atoms coupled via Feshbach resonances with a strength tunable by applying external magnetic fields, see Fig. 1. After the preparation of fermionic dimers in 2003, now also the BEC [1, 2] and superfluidity of these dimers has been observed [3, 4]. The BEC-BCS crossover is physically related [5] to the bound state dissociation or Mott-Anderson delocalization transition [6] where the modification of the effective coupling strength is caused by electronic screening and/or Pauli blocking effects [7]. It is thus a very general effect expected to

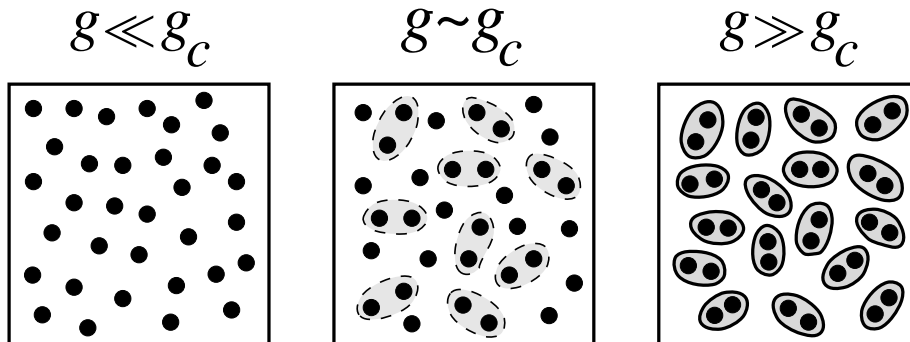


Figure 1: Illustration of the transition from BCS pairing with delocalized wave functions to BEC of bound states, well-localized in coordinate space, from Ref. [14]

occur in a wide variety of dense Fermi systems with attractive interactions [8] such as electron-hole systems in solid state physics [9], electron-proton systems in the interior of giant planets [10], deuterons in nuclear matter [11] or diquarks in quark matter [12]. The BEC-BCS crossover transition in quark matter is of particular theoretical interest due to the additional relativistic regime [13].

A systematic treatment of these effects is possible within the path integral formulation for finite-temperature quantum field theories. This approach is rather general as it is relativistic and is especially suited to take into account the effects of spontaneous symmetry breaking. Within these lectures we will present the basics of this approach on the example of a model field theory of the Nambu–Jona-Lasinio type for a relativistic strongly interacting Fermi system. These investigations are also motivated by the analogies of the strongly coupled quark-gluon plasma (sQGP) at Relativistic Heavy Ion Collider (RHIC) in Brookhaven [15] with the experiments on BEC of atoms in traps. Furthermore, qualitative insights into possible effects observable in the upcoming CBM experiment at FAIR Darmstadt as well as from neutron stars with quark matter interiors could be derived along the lines of this approach.

2 Path integral formalism

2.1 Partition function and model Lagrangian

As a generic model system for the description of hot, dense Fermi-systems with strong, short-range interactions we consider quark matter described by a model Lagrangian with four-fermion coupling. The key quantity for the derivation of thermodynamic properties is the partition function \mathcal{Z} from which all thermodynamic quantities can be derived. It is given as a path integral which in the imaginary time formalism ($t = -i\tau$) can be expressed as [16]

$$\mathcal{Z} = \int \mathcal{D}(iq^\dagger)\mathcal{D}(q) e^{\int^\beta d^4x (\mathcal{L} - \mu q^\dagger q)}, \quad (1)$$

where the chemical potential μ is introduced as a Lagrange multiplier for assuring conservation of baryon number as a conserved charge carried by the quarks. The notation $\int^\beta d^4x$ is shorthand for $\int_0^\beta d\tau \int d^3x$ where $\beta = 1/T$ is the inverse temperature. The quark matter is described by a Dirac Lagrangian with internal degrees of freedom ($N_f = 2$ flavors, $N_c = 3$ colors), with a current-current-type four-fermion interaction inspired by one-gluon exchange

$$\mathcal{L} = \bar{q}(i\cancel{\partial} - m_0)q - \frac{g^2}{2} \sum_{a=1}^8 \bar{q} \frac{\lambda^a}{2} \gamma_\mu q \bar{q} \frac{\lambda^a}{2} \gamma^\mu q, \quad (2)$$

where λ^a are the Gell-Mann matrices for color $SU(3)$. After Fierz transformation of the interaction, we select scalar diquark channel and the scalar and pseudoscalar channel so that our model Lagrangian assumes the form

$$\mathcal{L} = \mathcal{L}_0 + \mathcal{L}_{qq} + \mathcal{L}_{q\bar{q}} \quad (3)$$

where the different terms are given by

$$\mathcal{L}_0 = \bar{q}(i\cancel{\partial} - m_0)q \quad (4)$$

$$\mathcal{L}_{q\bar{q}} = G_S \left[(\bar{q}q)^2 + (\bar{q}i\gamma_5\tau q)^2 \right] \quad (5)$$

$$\mathcal{L}_{qq} = G_D \left\{ \bar{q} [i\gamma_5 C \tau_2 \lambda_2] \bar{q}^T \right\} \left\{ q^T [iC \gamma_5 \tau_2 \lambda_2] q \right\}, \quad (6)$$

where γ_ν are the Dirac matrices, τ_i are $SU(2)$ flavor matrices and $C = i\gamma^2\gamma^0$ is the charge conjugation matrix. G_S and G_D are the coupling strengths corresponding to the different channels, see Ref. [17] for a recent review. For the numerical analysis we adopt parameters from Ref. [18] and consider $\eta_D = G_D/G_S$ as a free parameter of the model.

A general method to deal with four-fermion interactions in the path integral approach starts with the Hubbard-Stratonovich transformation [19] of the partition function to its equivalent form in terms of collective bosonic fields, which is more suitable to deal with nonperturbative effects such as the occurrence of order parameters related to phase transitions in the system as well as collective excitations (plasmons = mesons and pairs = diquarks) in these phases.

2.2 Hubbard-Stratonovich transformation: Bosonization

The Hubbard-Stratonovich transformation is a two-step procedure which consists of (1) linearization of the four-fermion interaction terms by introducing bosonic auxiliary fields in the appropriate channels and (2) integrating out the fermions analytically.

We introduce the Hubbard-Stratonovich auxiliary fields $\Delta(\tau, x)$, $\Delta^*(\tau, x)$, $\pi(\tau, x)$ and $\sigma(\tau, x)$ so that the partition function of the system becomes

$$\begin{aligned} \mathcal{Z} = & \int \mathcal{D}\Delta^* \mathcal{D}\Delta \mathcal{D}\sigma \mathcal{D}\pi \left\{ e^{-\int^\beta d^4x \left[\frac{\sigma^2 + \pi^2}{4G_S} + \frac{|\Delta|^2}{4G_D} \right]} \right. \\ & \left. \times \int [dq] [d\bar{q}] e^{\int^\beta d^4x (\bar{q}(i\cancel{\partial} + \mu\gamma_0 - m_0)q - \bar{q}(\sigma + i\gamma_5\tau \cdot \pi)q - \frac{\Delta^*}{2} q^T R q - \frac{\Delta}{2} \bar{q} \bar{R} \bar{q}^T)} \right\}. \end{aligned} \quad (7)$$

where $R = iC\gamma_5 \otimes \tau_2 \otimes \lambda_2$, $\tilde{R} = i\gamma_5 C \otimes \tau_2 \otimes \lambda_2$. By introducing Nambu-Gorkov spinors

$$\Psi \equiv \frac{1}{\sqrt{2}} \begin{pmatrix} q \\ q^c \end{pmatrix}, \quad \bar{\Psi} \equiv \frac{1}{\sqrt{2}} (\bar{q}\bar{q}^c) \quad (8)$$

with $q^c(x) \equiv C\bar{q}^T(x)$, the Lagrangian takes the bilinear form

$$\mathcal{L} = \bar{\Psi} \begin{pmatrix} i\cancel{\partial} + \mu\gamma_0 - \hat{m} - i\gamma_5\boldsymbol{\tau} \cdot \boldsymbol{\pi} & i\Delta\gamma_5\tau_2\lambda_2 \\ i\Delta^*\gamma_5\tau_2\lambda_2 & i\cancel{\partial} - \mu\gamma_0 - \hat{m} - i\gamma_5\boldsymbol{\tau} \cdot \boldsymbol{\pi} \end{pmatrix} \Psi \quad (9)$$

with $\hat{m} = m_0 + \sigma$. Hence the partition function becomes a Gaussian path integral in the bispinor fields which can be evaluated and yields the fermion determinant

$$\mathcal{Z} = \int \mathcal{D}\Delta^* \mathcal{D}\Delta \mathcal{D}\sigma \mathcal{D}\boldsymbol{\pi} e^{-\int^\beta d^4x \frac{\sigma^2 + \boldsymbol{\pi}^2}{4G_S} + \frac{|\Delta|^2}{4G_D}} \int \mathcal{D}\bar{\Psi} \mathcal{D}\Psi e^{\int^\beta d^4x \bar{\Psi}[S^{-1}]\Psi} \quad (10)$$

$$= \int \mathcal{D}\Delta^* \mathcal{D}\Delta \mathcal{D}\sigma \mathcal{D}\boldsymbol{\pi} e^{-\int^\beta d^4x \frac{\sigma^2 + \boldsymbol{\pi}^2}{4G_S} + \frac{|\Delta|^2}{4G_D}} \cdot \text{Det}[S^{-1}], \quad (11)$$

where the inverse bispinor propagator is a matrix in Nambu-Gorkov-, Dirac-, color- and flavor space which after Fourier transformation reads

$$S^{-1} = \begin{pmatrix} (i\omega_n + \mu)\gamma_0 - \hat{m} - i\boldsymbol{\gamma}\mathbf{p} - i\gamma_5\boldsymbol{\tau} \cdot \boldsymbol{\pi} & i\Delta\gamma_5\tau_2\lambda_2 \\ i\Delta^*\gamma_5\tau_2\lambda_2 & (i\omega_n - \mu)\gamma_0 - \hat{m} - i\boldsymbol{\gamma}\mathbf{p} + i\gamma_5\boldsymbol{\tau} \cdot \boldsymbol{\pi} \end{pmatrix} \quad (12)$$

So far we could derive with (11) a very compact, bosonized form of the quark matter partition function (1) which is an exact transformation of (1), now formulated in terms of collective, bosonic fields. As we will demonstrate in the following, this form is suitable since it allows to obtain nonperturbative results already in the lowest orders with respect to an expansion around the stationary values of these fields. In performing this expansion, we may factorize the partition function into mean field (MF), Gaussian fluctuation (Gauss) and residual (res) contributions

$$\mathcal{Z}(\mu, T) \equiv e^{-\beta\Omega(\mu, T)} = Z_{MF}(\mu, T) Z_{\text{Gauss}}(\mu, T) Z_{\text{res}}(\mu, T).$$

In the following we will discuss the physical content of these approximations.

2.3 Mean-field approximation: order parameters

In thermodynamical equilibrium, the mean field values satisfy the stationarity condition of the minimal thermodynamical potential $\Omega_{MF} \equiv -\frac{1}{\beta V} \ln \mathcal{Z}_{MF}$, i.e.

$$\frac{\partial \Omega_{MF}}{\partial \sigma_{MF}} = \frac{\partial \Omega_{MF}}{\partial \boldsymbol{\pi}_{MF}} = \frac{\partial \Omega_{MF}}{\partial \Delta_{MF}} = 0, \quad (13)$$

equivalent to the fulfillment of the gap equations $\sigma_{MF} = -4G_S \text{Tr}(S_{MF}) \equiv m - m_0$, $\boldsymbol{\pi}_{MF} = -4iG_S \text{Tr}(\boldsymbol{\gamma}_5 \vec{\boldsymbol{\tau}} S_{MF}) = 0$ and $\Delta_{MF} = 4G_D \text{Tr}(\boldsymbol{\gamma}_5 \tau_2 \lambda_2 S_{MF}) = \Delta$, together with the stability criterion that the determinant of the curvature matrix

formed by the second derivatives is positive. After the evaluation of the traces in the internal spaces and the sum over the Matsubara frequencies one gets

$$\begin{aligned}
\Omega_{MF} &= -\frac{1}{\beta V} \ln \mathcal{Z}_{MF} = \frac{(m - m_0)^2}{4G_S} + \frac{|\Delta|^2}{4G_D} - \frac{1}{\beta V} \text{Tr} (\ln \beta S_{MF}^{-1}) \\
&= \frac{(m - m_0)^2}{4G_S} + \frac{|\Delta|^2}{4G_D} - 4 \int \frac{d^3 p}{(2\pi)^3} \left[E_{\mathbf{p}}^+ + E_{\mathbf{p}}^- + E_{\mathbf{p}} + 2T \ln(1 + e^{-\beta E_{\mathbf{p}}^+}) \right. \\
&\quad \left. + 2T \ln(1 + e^{-\beta E_{\mathbf{p}}^-}) + T \ln(1 + e^{-\beta \xi_{\mathbf{p}}^+}) + T \ln(1 + e^{-\beta \xi_{\mathbf{p}}^-}) \right] \quad (14)
\end{aligned}$$

where we have defined the particle dispersion relation $E_{\mathbf{p}}^{\pm} = \sqrt{(\xi_{\mathbf{p}}^{\pm})^2 + \Delta^2}$ with $\xi_{\mathbf{p}}^{\pm} = E_{\mathbf{p}} \pm \mu$, $E_{\mathbf{p}} = \sqrt{m^2 + \mathbf{p}^2}$. The $\Delta \neq 0$ dispersion law is associated to the red and green quarks ($E_{\mathbf{p}}^-$) and antiquarks ($E_{\mathbf{p}}^+$), whereas the ungapped blue quarks (antiquarks) have the dispersion $\xi_{\mathbf{p}}^-$ ($\xi_{\mathbf{p}}^+$). From Eqs. (13) with (14) we obtain the gap equations for the order parameters m and Δ , which have to be solved self-consistently,

$$\begin{aligned}
m - m_0 &= 8G_S m \int \frac{d^3 p}{(2\pi)^3} \frac{1}{E_{\mathbf{p}}} \left\{ [1 - 2n_F(E_{\mathbf{p}}^-)] \frac{\xi_{\mathbf{p}}^-}{E_{\mathbf{p}}} \right. \\
&\quad \left. + [1 - 2n_F(E_{\mathbf{p}}^+)] \frac{\xi_{\mathbf{p}}^+}{E_{\mathbf{p}}^+} + n_F(-\xi_{\mathbf{p}}^+) - n_F(\xi_{\mathbf{p}}^-) \right\}, \quad (15)
\end{aligned}$$

$$\Delta = 8G_D \int \frac{d^3 p}{(2\pi)^3} \left[\frac{1 - 2n_F(E_{\mathbf{p}}^-)}{E_{\mathbf{p}}^-} + \frac{1 - 2n_F(E_{\mathbf{p}}^+)}{E_{\mathbf{p}}^+} \right], \quad (16)$$

with the Fermi distribution function $n_F(E) = (1 + e^{\beta E})^{-1}$. For zero temperature, the gap equations take the simple form

$$m - m_0 = 8G_S m \int \frac{d^3 p}{(2\pi)^3} \frac{1}{E_{\mathbf{p}}} \left[\frac{\xi_{\mathbf{p}}^-}{E_{\mathbf{p}}} + \frac{\xi_{\mathbf{p}}^+}{E_{\mathbf{p}}^+} + \Theta(\xi_{\mathbf{p}}^-) \right], \quad (17)$$

$$\Delta = 8G_D \Delta \int \frac{d^3 p}{(2\pi)^3} \left[\frac{1}{E_{\mathbf{p}}^-} + \frac{1}{E_{\mathbf{p}}^+} \right]. \quad (18)$$

Solutions of the gap equations for the dynamically generated quark mass m and for the diquark pairing gap Δ at $T = 0$ as a function of the chemical potential are shown in Fig. 2. From the knowledge of the order parameters as functions of the thermodynamical variables (T, μ) we can deduce the phase diagram of Fig. 3.

2.4 Phase diagram

From the solutions of the gap equations for the order parameters in dependence of the thermodynamical variables T and μ we have constructed the phase diagram of the present quark matter model in the $T - \mu$ plane, see Fig. 3. The two order parameters allow to distinguish 4 phases:

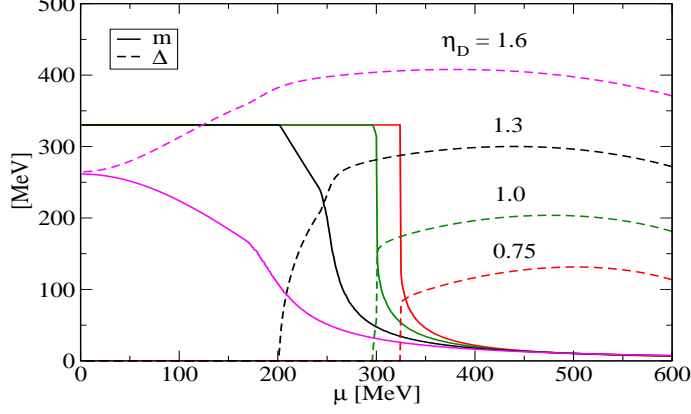


Figure 2: Order parameters for chiral symmetry breaking (full lines) and color superconductivity (dashed lines) at $T = 0$ for different values of the diquark coupling η_D . First order phase transitions turn to second order or even crossover when η_D is increased. For details, see text.

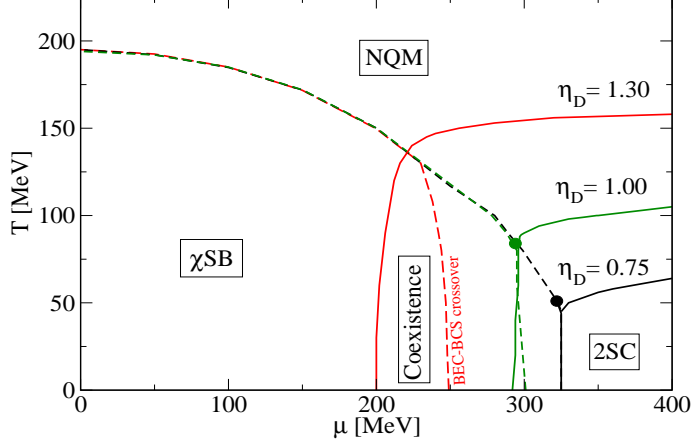


Figure 3: Phase diagram of two-flavor quark matter with critical lines for chiral symmetry breaking (dashed) and color superconductivity (solid) for three values of the diquark coupling strength: $\eta_D = 0.75$ (black), 1.0 (green) and 1.3 (red). The BEC-BCS crossover occurs when the chiral transition (coincident with the Mott transition for mesonic and diquark bound states) occurs inside the 2SC phase. It is characterized by the coexistence of diquark condensation with chiral symmetry breaking.

- $\Delta = 0, m \sim m_0$: normal phase (NQM)
- $\Delta \neq 0, m \sim m_0$: color superconductor (2SC)
- $\Delta = 0, m \gg m_0$: chiral symmetry broken phase (χ SB)
- $\Delta \neq 0, m \gg m_0$: coexistence of χ SB and 2SC (BEC phase)

Order parameters are indicators of phase transitions. The phase transitions can be classified according to their order, depending on the behavior of the order parameters with the change of thermodynamic variables

- first order: order parameter jumps, as in the case of the χ SB \rightarrow 2SC phase transition at not too large coupling.
- second order: order parameter turns continuously to zero. The 2SC \rightarrow NQM transition with increasing T is always second order. The χ SB \rightarrow 2SC transition turns from 1st to 2nd order for strong enough coupling.
- crossover: the order parameter changes continuously, but does not go to zero and also has no jumps. An example is the χ SB \rightarrow NQM transition at temperatures above the critical endpoint (CP) where it goes over to the line of 1st order transitions in the $T - \mu$ plane. The identification of the CP is a key issue for experimental research and thus for the verification of QCD models. It is suggested that verifiable signatures (change of the fluctuation spectrum, latent heat or not) are related with it. For strong coupling, the CP moves to lower T and finally to $T = 0$ (for $\eta_D > 1.3$ the chiral transition is always crossover).

Increasing the diquark coupling η_D leads to an increase of the diquark gap and therefore a rise in the critical temperature for the second order transition to a normal quark matter phase. It shifts also the border between color superconductivity (2SC) and chiral symmetry broken phase (χ SB) to lower values of the chemical potential. For very strong coupling $\eta_D \sim 1$, a coexistence region develops, where both order parameters are simultaneously nonvanishing. Under these conditions, the phase border is not of first order and therefore no critical endpoint can be identified. As we are going to explain in the next section, in the χ SB phase pion and diquark bound states can exist. At the chiral symmetry restoration transition, they merge the continuum of unbound states and turn into (resonant) scattering states. When this Mott transition occurs within the 2SC phase (characterized by a nonvanishing diquark condensate) we speak of a BEC-BCS crossover: the condensation of diquark bound states (BEC) turns into a condensation of resonances, called Cooper pairs (BCS).

For lower coupling, the critical point occurs and is shown as a colored dot in the phase diagram of Fig. 3.

In the next section we will turn towards the interesting question about the quasiparticle excitations in these phases. To this end, we will expand the action functional in the partition function up to quadratic (Gaussian) order in the mesonic fields and arrive at a tractable approximation for the bosonized quark matter model (11).

2.5 Gaussian fluctuations: bound & scattering states

Let us expand now the mesonic fields around their mean field values. In these lectures, we will focus on fluctuations in the mesonic channels, where the pion and the sigma meson will emerge as quasiparticle degrees of freedom. On the example of the pion we will explain the physics of the Mott transition. As discussed in the previous section, the phenomenon of the BEC-BCS crossover in the 2SC phase is due to the Mott transition for diquarks. The detailed investigation of the quantized diquark fluctuations, which are also a prerequisite of the formation of baryons, will be given elsewhere [?, 20]. As we already noticed, the pion does not contribute to the mean field, and we need to introduce only the sigma-field fluctuations as $\sigma \rightarrow \sigma_{MF} + \sigma$. Hence it is possible to decompose the inverse propagator S^{-1} into a mean field part and a fluctuation part $S^{-1} = S_{MF}^{-1} + \Sigma$, where the matrix Σ is defined as

$$\Sigma \equiv \begin{pmatrix} -\sigma - i\gamma_5 \vec{\tau} \cdot \vec{\pi} & 0 \\ 0 & -\sigma - i\gamma_5 \vec{\tau}^t \cdot \vec{\pi} \end{pmatrix}. \quad (19)$$

In the Gaussian approximation the fermion determinant becomes

$$\frac{\text{Det} [S^{-1}]|_{\text{Gauss}}}{\text{Det} [S_{MF}^{-1}]} = \exp \left\{ -\frac{1}{2} \int \frac{d^4q}{(2\pi)^4} \text{Tr} [S_{MF}(p)\Sigma(q)S_{MF}(p+q)\Sigma(q)] \right\}. \quad (20)$$

The propagator S_{MF} is obtained from (12) by the matrix inversion¹

$$S_{MF} \equiv \begin{pmatrix} \mathbf{G}^+ & \mathbf{F}^- \\ \mathbf{F}^+ & \mathbf{G}^- \end{pmatrix} \quad (21)$$

with the matrix elements

$$\mathbf{G}_p^\pm = \sum_{s_p} \sum_{t_p} \frac{t_p}{2E_{\mathbf{p}}^{\pm s_p}} \frac{t_p E_{\mathbf{p}}^{\pm s_p} - s_p \xi_{\mathbf{p}}^{\pm s_p}}{p_0 - t_p E_{\mathbf{p}}^{\pm s_p}} \Lambda_{\mathbf{p}}^{-s_p} \gamma_0 \mathcal{P}_{\text{rg}} + \sum_{s_p} \frac{\Lambda_{\mathbf{p}}^{-s_p} \gamma_0 \mathcal{P}_{\text{b}}}{p_0 + s_p \xi_{\mathbf{p}}^{\pm s_p}}, \quad (22)$$

$$\mathbf{F}_p^\pm = i \sum_{s_p} \sum_{t_p} \frac{t_p}{2E_{\mathbf{p}}^{\pm s_p}} \frac{\Delta^\pm}{p_0 - t_p E_{\mathbf{p}}^{\pm s_p}} \Lambda_{\mathbf{p}}^{s_p} \gamma_5 \tau_2 \lambda_2, \quad (23)$$

where $s_p, t_p = \pm 1$, $(\Delta^+, \Delta^-) = (\Delta^*, \Delta)$. For the subsequent evaluation of traces in quark-loop diagrams, it is convenient to use this notation with projectors in color space, $\mathcal{P}_{\text{rg}} = \text{diag}(1, 1, 0)$, $\mathcal{P}_{\text{b}} = \text{diag}(0, 0, 1)$ and in Dirac space,

$$\Lambda_{\mathbf{p}}^\pm = \frac{1}{2} \left[1 \pm \gamma_0 \left(\frac{\vec{\gamma} \cdot \vec{p} + \hat{m}}{E_{\mathbf{p}}} \right) \right].$$

The summation over Matsubara frequencies $p_0 = i\omega_n$ is most systematic using the above decomposition into simple poles in the p_0 plane. The poles of the normal propagators \mathbf{G}^\pm are given by the gapped dispersion relations for the paired red-green quarks (antiquarks), $E_{\mathbf{p}}^\pm = \sqrt{(\xi_{\mathbf{p}}^\pm)^2 + \Delta^2}$, and the ungapped dispersions $\xi_{\mathbf{p}}^\pm = E_{\mathbf{p}} \pm \mu$ for the blue quarks (antiquarks). The anomalous

¹contribution by M. Buballa

propagators $\mathbf{F}_{\mathbf{p}}^{\pm}$ are only nonvanishing in the 2SC phase when the pair amplitude is nonvanishing. Let us notice explicitly that this procedure has yielded an effective action that includes the fluctuation terms responsible for the excitation of scalar and pseudoscalar mesonic modes. The evaluation of the traces (20) can be performed with the result

$$\frac{1}{2}\text{Tr}(S_{MF}\Sigma S_{MF}\Sigma) = (\vec{\pi}, \sigma) \begin{pmatrix} \Pi_{\pi\pi} & 0 \\ 0 & \Pi_{\sigma\sigma} \end{pmatrix} \begin{pmatrix} \vec{\pi} \\ \sigma \end{pmatrix} \quad (24)$$

with

$$\Pi_{\sigma\sigma}(q_0, \mathbf{q}) \equiv \text{Tr}[\mathbf{G}_p^+ \mathbf{G}_{p+q}^+ + \mathbf{F}_p^- \mathbf{F}_{p+q}^+ + \mathbf{G}_p^- \mathbf{G}_{p+q}^- + \mathbf{F}_p^+ \mathbf{F}_{p+q}^-] \quad (25)$$

$$\begin{aligned} \Pi_{\pi\pi}(q_0, \mathbf{q}) \equiv & -\text{Tr}[\mathbf{G}_p^+(\gamma_5 \vec{\tau}) \mathbf{G}_{p+q}^+(\gamma_5 \vec{\tau}) + \mathbf{F}_p^-(\gamma_5 \vec{\tau}^t) \mathbf{F}_{p+q}^+(\gamma_5 \vec{\tau}) \\ & + \mathbf{F}_p^+(\gamma_5 \vec{\tau}) \mathbf{F}_{p+q}^-(\gamma_5 \vec{\tau}^t) + \mathbf{G}_p^-(\gamma_5 \vec{\tau}^t) \mathbf{G}_{p+q}^-(\gamma_5 \vec{\tau}^t)]. \end{aligned} \quad (26)$$

These polarization functions are the key quantities for the investigation of mesonic bound and scattering states in quark matter. In the following we perform the further evaluation and discussion for the pionic modes, the σ modes is treated in an analogous way. We start with the evaluation of traces and Matsubara summation.

$$\begin{aligned} \Pi_{\pi\pi}(q_0, \mathbf{q}) = & 2 \int \frac{d^3p}{(2\pi)^3} \sum_{s_p, s_k} \mathcal{T}_-^+(s_p, s_k) \left\{ \frac{n_F(s_p \xi_{\mathbf{p}}^{s_p}) - n_F(s_k \xi_{\mathbf{p}+\mathbf{q}}^{s_k})}{q_0 - s_k \xi_{\mathbf{p}+\mathbf{q}}^{s_k} + s_p \xi_{\mathbf{p}}^{s_p}} \right. \\ & + \frac{n_F(s_p \xi_{\mathbf{p}}^{s_p}) - n_F(s_k \xi_{\mathbf{p}+\mathbf{q}}^{s_k})}{q_0 + s_k \xi_{\mathbf{p}+\mathbf{q}}^{s_k} - s_p \xi_{\mathbf{p}}^{s_p}} + \sum_{t_p, t_k} \frac{t_p t_k}{E_{\mathbf{p}}^{s_p} E_{\mathbf{p}+\mathbf{q}}^{s_k}} \frac{n_F(t_p E_{\mathbf{p}}^{s_p}) - n_F(t_k E_{\mathbf{p}+\mathbf{q}}^{s_k})}{q_0 - t_k E_{\mathbf{p}+\mathbf{q}}^{s_k} + t_p E_{\mathbf{p}}^{s_p}} \\ & \left. \times (t_p t_k E_{\mathbf{p}}^{s_p} E_{\mathbf{p}+\mathbf{q}}^{s_k} + s_p s_k \xi_{\mathbf{p}}^{s_p} \xi_{\mathbf{p}+\mathbf{q}}^{s_k} - |\Delta|^2) \right\} \end{aligned} \quad (27)$$

where

$$\mathcal{T}_-^+(s_p, s_k) = \left(1 + s_p s_k \frac{\mathbf{p} \cdot (\mathbf{p} + \mathbf{q}) - m^2}{E_{\mathbf{p}} E_{\mathbf{p}+\mathbf{q}}} \right). \quad (28)$$

For a pionic mode at rest in the medium ($\mathbf{q} = 0$) this reduces to

$$\begin{aligned} \Pi_{\pi\pi}(q_0, \mathbf{0}) = & 8 \int \frac{d^3p}{(2\pi)^3} \left\{ N(\xi_{\mathbf{p}}^+, \xi_{\mathbf{p}}^-) \left[\frac{1}{q_0 - 2E_{\mathbf{p}}} - \frac{1}{q_0 + 2E_{\mathbf{p}}} \right] \right. \\ & + \left[1 - \frac{\xi_{\mathbf{p}}^+ \xi_{\mathbf{p}}^- + \Delta^2}{E_{\mathbf{p}}^+ E_{\mathbf{p}}^-} \right] M(E_{\mathbf{p}}^+, E_{\mathbf{p}}^-) \left[\frac{1}{q_0 - E_{\mathbf{p}}^+ + E_{\mathbf{p}}^-} - \frac{1}{q_0 + E_{\mathbf{p}}^+ - E_{\mathbf{p}}^-} \right] \\ & \left. + \left[1 + \frac{\xi_{\mathbf{p}}^+ \xi_{\mathbf{p}}^- + \Delta^2}{E_{\mathbf{p}}^+ E_{\mathbf{p}}^-} \right] N(E_{\mathbf{p}}^+, E_{\mathbf{p}}^-) \left[\frac{1}{q_0 - E_{\mathbf{p}}^+ - E_{\mathbf{p}}^-} - \frac{1}{q_0 + E_{\mathbf{p}}^+ + E_{\mathbf{p}}^-} \right] \right\} \end{aligned} \quad (29)$$

where we have introduced the phase space occupation factors $N(x, y) = 1 - n_F(x) - n_F(y)$ (Pauli blocking) and $M(x, y) = n_F(x) - n_F(y)$. For $\mu \neq 0$ this function has three poles from the first terms in each bracket, corresponding to positive energies ($q_0 > 0$). So we need to focus only on these three terms. For

$\mu = 0$ the second term vanishes due to the prefactor and we are left with two poles.

We make use of the Dirac identity $\lim_{\eta \rightarrow 0} \frac{1}{x+i\eta} = \mathcal{P}\frac{1}{x} - i\pi\delta(x)$ in order to decompose the polarization function into real and imaginary parts after analytical continuation to the complex plane. The imaginary part is straightforwardly integrated after transformation from momentum to energy ω . At the pole the variables transform as

$$p_\omega = \sqrt{\frac{\omega^4 - 4\omega^2(\mu^2 + \Delta^2)}{4(\omega^2 - 4\mu^2)} - m^2}. \quad (30)$$

For $\eta_D < 1$ we know that $\Delta = 0$ if $m \geq \mu$, what includes that $\omega \geq 2\mu$ as this is the relevant threshold. Therefore, the pole is not hidden and we recover the usual $2m$ threshold. For small enough couplings, $\Delta \neq 0$ only if $m < \mu$. Therefore, this pole is not hidden in this case. This reasoning includes that the argument of the square root is strictly positive. The integration borders thus shift $p \in (0, \infty) \rightarrow \omega \in (X_\pm, \infty)$, where the thresholds are given by $2m$ and

$$X_\pm = \sqrt{(m + \mu)^2 + \Delta^2} \pm \sqrt{(m - \mu)^2 + \Delta^2}. \quad (31)$$

The pion polarization function in the 2SC phase can thus be decomposed into real and imaginary parts in the following form

$$\begin{aligned} \Pi_{\pi\pi}^\Delta(\omega + i\eta, \mathbf{0}) &= \mathbf{Re}\Pi_{\pi\pi}^\Delta(\omega + i\eta, \mathbf{0}) + i\mathbf{Im}\Pi_{\pi\pi}^\Delta(\omega + i\eta, \mathbf{0}) \\ &= 8 \int \frac{d^3p}{(2\pi)^3} \left\{ N(\xi_{\mathbf{p}}^+, \xi_{\mathbf{p}}^-) \left[\frac{\mathcal{P}}{\omega - 2E_{\mathbf{p}}} - \frac{1}{\omega + 2E_{\mathbf{p}}} \right] \right. \\ &\quad + \left[1 - \frac{\xi_{\mathbf{p}}^+ \xi_{\mathbf{p}}^- + \Delta^2}{E_{\mathbf{p}}^+ E_{\mathbf{p}}^-} \right] M(E_{\mathbf{p}}^+, E_{\mathbf{p}}^-) \left[\frac{\mathcal{P}}{\omega - E_{\mathbf{p}}^+ + E_{\mathbf{p}}^-} - \frac{1}{\omega + E_{\mathbf{p}}^+ - E_{\mathbf{p}}^-} \right] \\ &\quad + \left. \left[1 + \frac{\xi_{\mathbf{p}}^+ \xi_{\mathbf{p}}^- + \Delta^2}{E_{\mathbf{p}}^+ E_{\mathbf{p}}^-} \right] N(E_{\mathbf{p}}^+, E_{\mathbf{p}}^-) \left[\frac{\mathcal{P}}{\omega - E_{\mathbf{p}}^+ - E_{\mathbf{p}}^-} - \frac{1}{\omega + E_{\mathbf{p}}^+ + E_{\mathbf{p}}^-} \right] \right\} \\ &\quad - i \frac{2}{\pi} \left\{ p_\omega^0 E_{p_\omega^0} N(\xi_{p_\omega^0}^+, \xi_{p_\omega^0}^-) \Theta(\omega - 2m) \right. \\ &\quad + p_\omega E_{p_\omega} \frac{E_{p_\omega}^+ E_{p_\omega}^- - \xi_{p_\omega}^+ \xi_{p_\omega}^- - \Delta^2}{\xi_{p_\omega}^+ E_{p_\omega}^- - \xi_{p_\omega}^- E_{p_\omega}^+} M(E_{p_\omega}^+, E_{p_\omega}^-) \Theta(\omega - X_-) \\ &\quad + \left. p_\omega E_{p_\omega} \frac{E_{p_\omega}^+ E_{p_\omega}^- + \xi_{p_\omega}^+ \xi_{p_\omega}^- + \Delta^2}{\xi_{p_\omega}^+ E_{p_\omega}^- + \xi_{p_\omega}^- E_{p_\omega}^+} N(E_{p_\omega}^+, E_{p_\omega}^-) \Theta(\omega - X_+) \right\} \end{aligned} \quad (32)$$

where \mathcal{P} denotes the principal value integration, $p_\omega^0 = p_\omega |_{\Delta=0} = \sqrt{\frac{\omega^2}{4} - m^2}$ and we have made explicit the three thresholds, $2m$ and X_\pm , for the occurrence of the corresponding decay processes giving rise to the partial widths Γ_{2m} and Γ_\pm , respectively. In the normal phase this reduces to

$$\begin{aligned} \Pi_{\pi\pi}^0(\omega + i\eta, \mathbf{0}) &= \mathbf{Re}\Pi_{\pi\pi}^0(\omega + i\eta, \mathbf{0}) + i\mathbf{Im}\Pi_{\pi\pi}^0(\omega + i\eta, \mathbf{0}) \\ &= 24 \int \frac{d^3p}{(2\pi)^3} N(\xi_{\mathbf{p}}^+, \xi_{\mathbf{p}}^-) \left[\frac{\mathcal{P}}{\omega - 2E_{\mathbf{p}}} - \frac{1}{\omega + 2E_{\mathbf{p}}} \right] \\ &\quad - i \frac{6}{\pi} p_\omega^0 E_{p_\omega^0} N(\xi_{p_\omega^0}^+, \xi_{p_\omega^0}^-) \Theta(\omega - 2m) \end{aligned} \quad (33)$$

The analytic properties of the mesonic modes can be analyzed from their spectral function. Here we discuss results for pionic modes with $\mathbf{q} = \mathbf{0}$ in the rest frame of the medium

$$\rho_\pi(\omega + i\eta, \mathbf{0}) = \frac{8G_\sigma^2 \mathbf{Im}\Pi_{\pi\pi}(\omega + i\eta, \mathbf{0})}{[1 - 2G_\sigma \mathbf{Re}\Pi_{\pi\pi}(\omega, \mathbf{0})]^2 + [2G_\sigma \mathbf{Im}\Pi_{\pi\pi}(\omega + i\eta, \mathbf{0})]^2} . \quad (34)$$

In the limit of vanishing imaginary part, we recover the spectral function for a “true” (on-shell) bound state

$$\lim_{\mathbf{Im}\Pi_{\pi\pi} \rightarrow 0} \rho_\pi(\omega + i\eta, \mathbf{0}) = 2\pi\delta(1 - 2G_\sigma \mathbf{Re}\Pi_{\pi\pi}(\omega, \mathbf{0})) , \quad (35)$$

which corresponds to an infinite lifetime of the state and a mass to be found from the pole condition $1 - 2G_\sigma \mathbf{Re}\Pi_{\pi\pi}(m_\pi, \mathbf{0}) = 0$. In Fig. 4, we show results for the mass spectrum of pions and sigma-mesons as a function of the temperature for vanishing chemical potential $\mu_B = 0$ and strong diquark coupling $\eta_D = 1.0$. Since $\Delta = 0$, the only threshold for the imaginary parts of meson decays is $2m$. The σ mass is always above the threshold and therefore this state is unstable in the present model. The pion, however, is a bound state until the critical temperature for the Mott transition $T_{\text{Mott}} = 212.7$ MeV is reached. For $T > T_{\text{Mott}}$ the pion becomes unstable for decay into quark-antiquark pairs. As can be seen from the behavior of the spectral function in the lower panel of Fig. 4, the pion is still a well-identifiable, long-lived resonance in that case. The detailed analytic behavior of the pion at the Mott transition has been discussed in the context of the NJL model by Hufner et al. [21], see also the inset of the lower panel of Fig. 4. It shows strong similarities with the behavior of bound states of fermionic atoms in traps when their coupling is tuned by exploiting Feshbach resonances in an external magnetic field, see [22]. In the context of RHIC experiments, one has discussed such quasi-bound states as an explanation for the perfect liquid behavior of the sQGP [23].

Next we want to discuss the pionic excitations in the presence of a diquark condensate in the 2SC phase, see Fig. 4. We choose $\mu = 320$ MeV and discuss the effect of melting the 2SC diquark condensate by increasing the temperature from $T = 0$ to $T > T_c$, where $T_c = 95$ MeV is the critical temperature for the second order transition to the normal quark matter phase. We observe the remarkable fact that the 2SC condensate stabilizes the pion at $T = 0$ as a true bound state, although the pion mass exceeds by far the threshold $2m$. This effect is due to a compensation of gapped and ungapped quark modes and has been discussed before by Ebert et al. [20] for $T = 0$ only. Here we extend this study to the finite temperature case, where the pion is still a very good resonance, but obtains a finite width. At the critical temperature T_c , the normal pion width is restored. But already before $T = T_c$ is reached, the threshold X_- is reached and the corresponding decay process is opened with a considerable width of $\mathcal{O}(50)$ MeV). From the pion spectral function in the lower panel of Fig. 4 we observe the gap in the excitation spectrum due to the presence of the diquark gap. At $T > T_c$, a resonance type spectral function with a threshold at $\omega = 2m$ and a resonance peak at $\omega \sim 250$ MeV is obtained.

The discussion of the mesonic modes in the 2SC phase points to a very rich spectrum of excitations which eventually lead to specific new observable signals

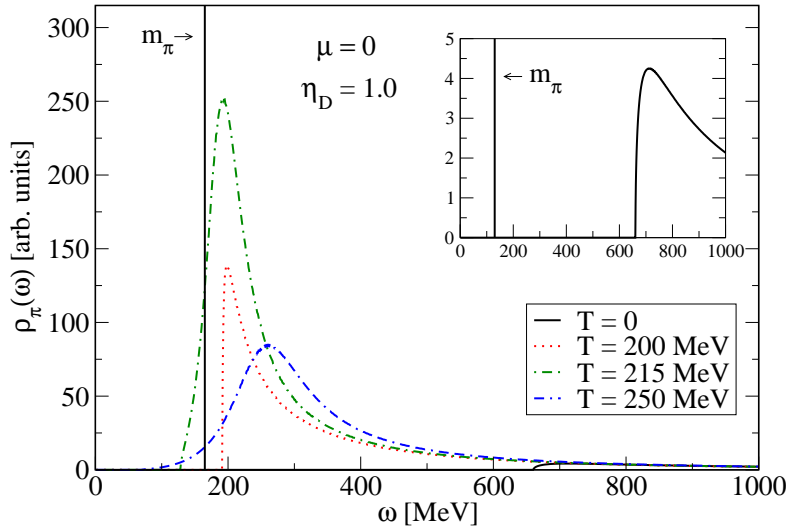
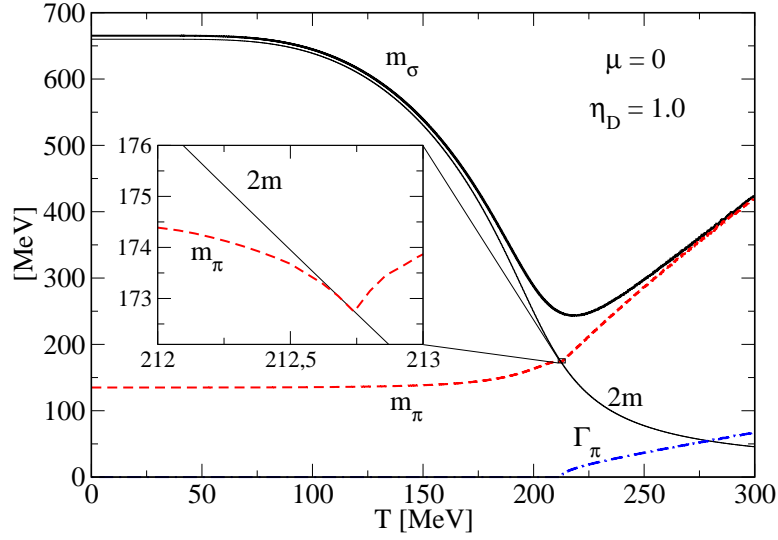


Figure 4: *Upper panel:* Mass spectrum of mesons (π , σ) as a function of the temperature for vanishing chemical potential $\mu_B = 0$ and strong diquark coupling $\eta_D = 1.0$. The threshold $E_{\text{th}} = 2 m_q$ for Mott dissociation of pions and occurrence of a nonvanishing decay width $\Gamma_\pi = \text{Im} \Pi_\pi/m_\pi$ is reached at $T_{\text{Mott}} = 212.7$ MeV (see inset). *Lower panel:* Spectral function for pionic correlations for $\mu_B = 0$ in the vacuum at $T = 0$ (see inset) and at different temperatures around the Mott transition. Below T_{Mott} , the bound state (delta function) and the continuum of scattering states are separated by a mass gap. Above T_{Mott} , the spectral function is still sharply peaked, related to a lifetime of pionic correlations of the order of the lifetime of a fireball in heavy-ion collisions (quasi-bound states in the quark plasma).

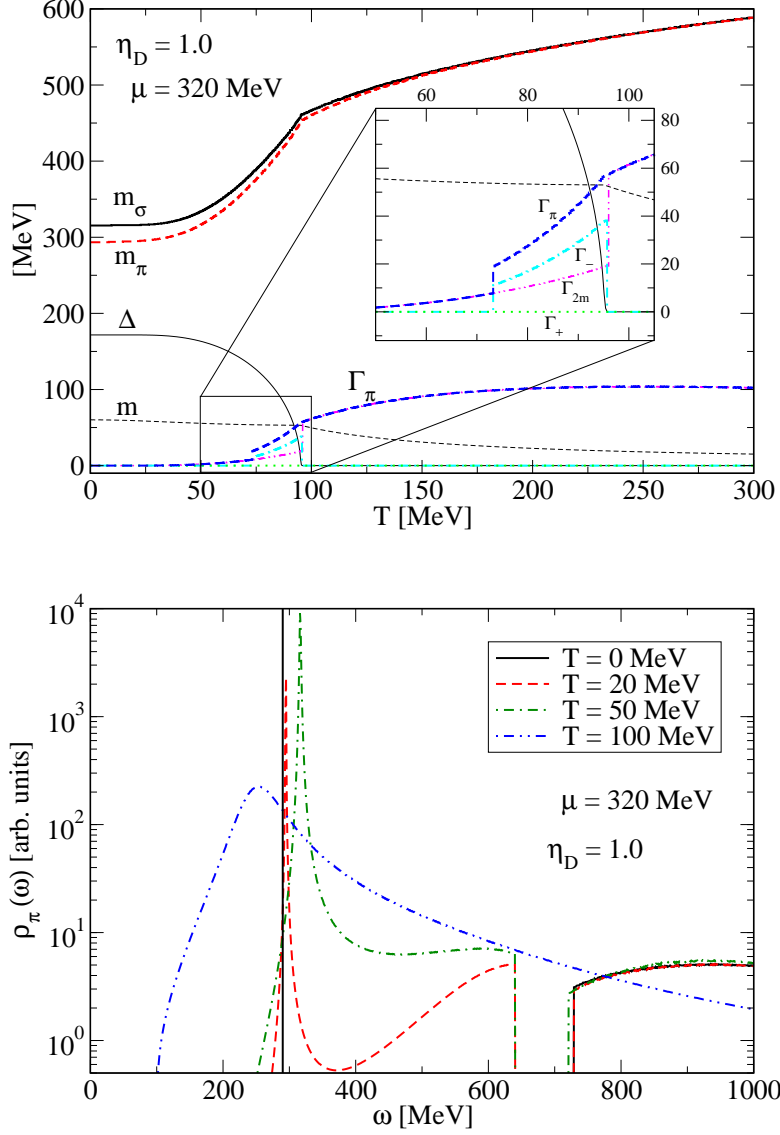


Figure 5: *Upper panel:* Mass spectrum of mesons (π , σ) as a function of the temperature for finite chemical potential $\mu_B = 320$ MeV and strong diquark coupling $\eta_D = 1.0$ in the 2SC phase. Below the threshold $E_{\text{th}} = 2 m_q$ for the onset of the decay width Γ_{2m} there is another process due to the lower threshold $E_+ - E_-$ switching on (see inset). *Lower panel:* Spectral function for pionic correlations for $\mu_B = 320$ in the 2SC phase at $T = 0$ and at different temperatures around the critical temperature for the 2SC phase.

of this hypothetical phase. The CBM experiment² planned at FAIR Darmstadt and the NICA project³ at JINR Dubna could be capable of creating thermodynamical conditions for the observation of these excitations in the experiment. In view of this discovery potential, we want to outline a few points for the further development of the theoretical approach.

3 Further Developments

In this contribution we have described the first steps into the interesting and very complex physics of the relativistic BEC-BCS crossover theory. As the next steps following this development, some of the approximations can be removed. In particular, one should next

- evaluate the full spectrum of diquark states, including their mixing with mesonic channels
- study the backreaction of the correlations on the meanfield (selfconsistent meanfield)
- include higher orders in the one-fermion-loop approximation (diquark-diquark and diquark-meson interactions)
- study the effect of the color neutrality condition by adjusting color chemical potential(s)
- study the effect of charge neutrality (gapless superconductivity)
- evaluate the contribution from diquark-antidiquark annihilation to the photon propagator (Maki-Thompson and Aslamasov-Larkin terms).

In particular the latter point bears a big potential for applications to the diagnostics of dense quark matter formed, e.g., in not too high- energy nucleus-nucleus collisions. The onset of color superconductivity not only changes the spectrum of diquark states (occurrence of the Goldstone bosons) but due to the nonvanishing diquark gap additional terms for the diquark annihilation process into the observable dilepton channel arise which stem from the nonvanishing anomalous propagator contributions. Since the critical temperature for the color superconductivity transition might be as high as 100 MeV there is a fair chance to observe traces of this transition with the future CBM experiment at FAIR Darmstadt.

4 Conclusions

We have derived the gap equations and Bethe-Salpeter equations for the simultaneous treatment of quantized density fluctuations (particle-antiparticle modes = mesons) in RPA approximation (one-fermion-loop polarization function) and quantized pairing fluctuations (particle-particle modes = diquarks) in ladder approximation (no crossed-ladder or vertex corrections) within the path integral

²contribution by P. Senger

³contribution by A.S. Sorin et al.

formalism, i.e. a fully relativistic field theoretical treatment. For the a priori unknown interaction, a local current-current coupling (NJL model) has been used which in the nonrelativistic limit becomes equivalent to the BCS model of superconductivity. After fixing the parameters of the model to the light meson spectrum in the vacuum, the diquark coupling remains as a free parameter which has been used to extend the model beyond the traditional range of applications into the region of BEC-BCS crossover, where both diquark bound states and scattering states occur simultaneously and determine the physical properties of the system. Recently, the tuning of the coupling in (nonrelativistic) low-temperature systems of fermionic atoms with Feshbach resonances in an external magnetic field could be used to investigate the BEC-BCS crossover in the laboratory. The nonrelativistic limit of the present approach can be used to interpret such results within a local coupling model. The fully relativistic form can be applied to model strong coupling QCD and to investigate the effects of finite temperature and density on the phase structure. We have presented in this contribution the phase diagram of quark matter at strong and very strong coupling, delineating a possible region of BEC-BCS crossover. The origin of the BEC-BCS crossover in superconducting quark matter is the Mott transition for diquark bound states. We explain the physics of the Mott transition on the example of mesonic correlations. We investigate the spectral function for pionic correlations (bound and scattering states) outside ($T > T_c$) and for the first time also inside ($T < T_c$) the color superconductivity region. We find the thresholds for the dissociation of pionic bound states into unbound, but resonant scattering states in the quark-antiquark continuum. For the lifetime of pionic resonances in the quark matter phase diagram see [24]. Summarizing, we have provided the framework for a study of hot and dense fermion matter beyond the mean field within a fully relativistic approach, with yet local interaction and in Gaussian approximation. The applications to QCD matter within a NJL model provide us with a phase diagram for quark matter which is now augmented with information about the presence of strong mesonic and diquark correlations with possible consequences in the phenomenology of relativistic heavy-ion collisions and the interiors of compact stars.

References

- [1] Greiner M, Regal C.A. and Jin D. S. // Nature 2003 V.426.P.537.
- [2] Zwierlein M. W., Stan C. A., Schunck C. H., Raupach S. M., Gupta S., Hadzibabic Z. and Ketterle W. // Phys. Rev. Lett. 2003 V.91.P.250401.
- [3] Zwierlein M. W., Abo-Shaeer J. R., Schirotzek A., Schunck C. H. and Ketterle W. // Nature 2003 V.435.P.1047.
- [4] Greiner M., Mandel O., Rom T., Altmeyer A., Widera A., Hänsch T. W. and Bloch I. // Physica B 2003 V.329.P.11.
- [5] Calzetta E., Hu B. L. and Rey A. M. // Phys. Rev. A 2006 V.73.P.023610.
- [6] Mott N. // Rev. Mod. Phys. 1968 V.40.P.677

- [7] *Ebeling W. et al.* // arXiv:0810.3336 [physics.plasma-ph]
- [8] *Sedrakian A., Clark J. W. and Alford M. (Eds.)* // *Pairing in fermionic systems*, World Scientific (2006)
- [9] *Bronold F. X. and Fehske H.* // Phys. Rev. B 2006 V.74.P.165107.
- [10] *Redmer R. et al.*, // J. Phys. A 2006 V.39.P.4479.
Nettelmann N. et al., // Astrophys. J. 2008 V.683.P.1217.
- [11] *Schmidt M., Röpke G. and Schulz H.* // Ann. Phys. 1990 V.202.P.57.
Stein H., Schnell A., Alm T., and Röpke G. // Z. Phys. A 1995 V.351.P.295.
Schnell A., Röpke G. and Schuck P. // Phys. Rev. Lett. 1999 V.83.P.1926.
- [12] *Kitazawa M., Koide T., Kunihiro T. and Nemoto Y.* // Phys. Rev. D 2002 V.65.P.091504.
Kitazawa M., Koide T., Kunihiro T. and Nemoto Y. // Phys. Rev. D 2004 V.70.P.056003.
Blaschke D., Ebert D., Klimenko K. G., Volkov M. K. and Yudin V. L. // Phys. Rev. D 2004 V.70.P.014006.
Blaschke D., Fredriksson S., Grigorian H., Öztas A.M. and Sandin F. // Phys. Rev. D 2005 V.72.P.065020.
- [13] *Abuki H.* // Nucl. Phys. A 2007 V.791.P.117.
Deng J., Schmitt A. and Wang Q. // Phys. Rev. D 2007 V.76.P.034013.
Sun G., He L. and Zhuang P. // Phys. Rev. D 2007 V.75.P.096004.
- [14] *Chen Q., Stajic J. and Levin K.* // J. Low Temp. Phys. 2005 V.32.P.406.
- [15] *Shuryak E. V.* // arXiv:nucl-th/0606046.
- [16] *Kapusta J.* // *Finite-temperature Field Theory*, Cambridge University Press (1989) P.26
- [17] *Buballa M.* // Phys. Rept. 2005 V.407.P.205.
- [18] *Grigorian H.* // Phys. Part. Nucl. Lett. 2007 V. 4.P.223
- [19] *Kleinert, H.* // Fortsch. Phys. 1978 V.26.P.565.
- [20] *Ebert D., Klimenko K. G. and Yudin V. L.* // Phys. Rev. C 2005 V.72.P.015201.
- [21] *Hüfner J., Klevansky S. P. and Rehberg P.* // Nucl. Phys. A 1996 V.606.P.260.
- [22] *Gurarie V. and Radzihovsky L.* // Ann. Phys. 2007 V.322.P.2.
- [23] *Shuryak E. V. and Zahed I.* // Phys. Rev. D 2004 V.70.P.054507.
- [24] *Zablocki D., Blaschke D. and Anglani R.* // AIP Conf. Proc. 2008 V.1038.P.159.